

Quantum Dynamics of the Avian Compass

Zachary B. Walters¹

¹*Max Planck Institute for Physics of Complex Systems,
Nöthnitzer Strasse 38, D-01187 Dresden, Germany*

(Dated: August 14, 2012)

The ability of migratory birds to orient relative to the Earth's magnetic field is believed to involve a coherent superposition of two spin states of a radical electron pair. However, the mechanism by which this coherence can be maintained in the face of strong interactions with the cellular environment has remained unclear. This Letter addresses the problem of decoherence between two electron spins due to hyperfine interaction with a bath of spin 1/2 nuclei. Conditions necessary for long lived coherence are identified, and a simple yet robust model for sensing magnetic field orientation is presented.

The ability of a migratory bird to orient itself relative to the Earth's magnetic field is at once a familiar feature of everyday life and a puzzling problem of quantum mechanics. That birds have this ability is well established by a long series of behavioral experiments. However, the precise mechanism by which an organism may sense the orientation of the weak geomagnetic field remains unclear and theoretically problematic.

Although commonly referred to as the "avian compass," the ability to sense the local magnetic field orientation has been observed in every major group of vertebrates, as well as crustaceans, insects, and a species of mollusc [1, 2]. For the majority of species, the primary compass mechanism appears to be light-activated, with only a few exceptions such as the sea turtle or the subterranean mole rat[2]. In addition to a light-activated compass located in the eye, migratory birds are believed to possess a separate mechanism involving magnetite, with possible receptors identified in the beak[3], the middle ear[4] and the brain stem[5]. This paper addresses the light-activated mechanism, which in addition to being widespread is also well studied by a long series of behavioral experiments, reviewed in [2, 6–9].

The basic parameters of the compass mechanism can be mapped out by confining a migratory bird in a conical cage during the preferred migration time. The restless nocturnal hopping behavior, or Zugunruhe, will then tend to orient itself in the preferred migratory direction. The importance of various environmental features can then be tested by observing their effects on the bird's ability to orient. Experiments along these lines have shown that the primary compass mechanism is light activated, with monochromatic 424 nm (blue) and 565 nm (green) light sufficient to orient, but with an abrupt transition to disoriented behavior between 560.5 nm and 567.5 nm. Under low irradiance 617.0 nm red light, birds showed oriented behavior rotated $\pm 90^\circ$ relative to the preferred orientation, behavior which was also observed at high irradiance with 565 nm light. [1, 2] This has been interpreted as indicating multiple light-activated receptors, with a high efficiency, short wavelength receptor yielding the correct orientation and a low efficiency,

long wavelength receptor yielding the rotated orientation. Doubling the magnetic field causes temporary disorientation lasting approximately an hour but correct orientation thereafter[10], showing that the compass mechanism can adapt to various magnetic field strengths, but that this adaptation is not instantaneous.

Experiments [11] with oscillating magnetic fields have shed light upon the quantum mechanical nature of the avian compass. Here the birds were subjected to a weak oscillatory field oriented transverse to the static field. When the frequency of oscillation was narrowly tuned to the Larmor frequency for an electron in a static field to flip its spin, the birds became disoriented, even when the oscillatory field strength (15 nT) was extremely weak relative to the static field strength (46 μ T). When the static field strength was doubled, so too was the frequency needed to disorient the birds. These results have been interpreted as lending support to a "radical pair" model, in which the field orientation is sensed via its effect upon two unpaired electron spins.

As originally formulated in [12, 13], the radical pair model holds that the absorption of a photon creates an excited state of two unpaired electrons initially in the $|s, m_s\rangle = |0, 0\rangle$ singlet state $|s\rangle$ (or, with identical logic, the $|s, m_s\rangle = |1, 0\rangle$ triplet state $|t\rangle$). Interaction with the local magnetic field then drives coherent oscillation between the singlet and triplet states with frequency $\omega = B_z \Delta\mu$. If the singlet and triplet states react at rates k_s and k_t to form distinguishable byproducts, the detection of these byproducts constitutes a probe of the quantum state [14] and, indirectly, of the field. If $k = k_s + k_t$, the fraction of triplet byproducts is given by

$$\text{triplet fraction} = \frac{k^2}{k^2 + \omega^2}. \quad (1)$$

While the radical pair model does an excellent job of explaining the broad features of behavioral experiments, it has both practical and theoretical difficulties. As a practical problem, the control signal given by Eq. 1 is weak unless k and ω are closely balanced. However, doubling the local field strength yields only temporary disorientation, while birds in the wild can adapt to local

field strengths ranging from 30 μT at the equator to 60 μT at the poles[15].

A more fundamental difficulty with the radical pair model is the need to maintain spin coherence in an environment which is extremely hostile to it. In a cellular environment, every water molecule possesses two spin 1/2 protons, which interact with unpaired electrons via the hyperfine interaction. However, as observed in [16], coherence between electrons must be maintained for 10^{-4} s or longer, or else the rate of spin flips due to an oscillatory field in [11] would be too low to affect the signal. Thus, understanding the avian compass requires an understanding of decoherence induced by the hyperfine interaction. In [17], this interaction was converted to an effective magnetic field, while [14] considered the effects of spin relaxation on the radical pair model. [18] propagated a system of two electrons interacting with several nuclear spins, finding that coherence between the electrons enhanced the sensitivity to magnetic field orientation. The related problem of electron spins in a quantum dot has been studied in [19, 20].

This paper addresses the problem of a two spin system in the $m_s = 0$ subspace, where decoherence is induced by hyperfine interactions with a bath of spin 1/2 nuclei. The form of this decoherence is found to differ if the electrons interact primarily with the same nuclei (proximate electrons) or with different sets of nuclei (distant electrons), or if the electrons interact with the same nuclei with the same or different strengths. The limit of closely spaced electrons is found to support long lived coherence, in a manner directly analogous to coherences in photosynthetic complexes[21]. Finally, this analysis is used to propose a new version of the radical pair model, which gives a biologically useful signal in the limit of strong interactions between the system and the bath, and gives a simple explanation of many behavioral experiments.

The Hamiltonian for a system of electronic spins \vec{S}_i and nuclear spins \vec{I}_k in an external field \vec{B} is given by [22]

$$H = \sum_i \mu_B \vec{B} \cdot \vec{S}_i + \vec{V}_{\text{SR}}^{(i)} \cdot \vec{S}_i + \sum_k \mu_I \vec{B} \cdot \vec{I}_k + \sum_{i,k} \frac{\mu_0}{4\pi} (2\mu_B \frac{\mu_I}{I}) \vec{I}_k \cdot [\frac{\vec{L}_i}{|r_{ik}|^3} - \frac{1}{|r_{ik}|^3} (\vec{S}_i - \frac{3(\vec{S}_i \cdot \vec{r}_{ik})\vec{r}_{ik}}{|r_{ik}|^2})] + \frac{8\pi}{3} |\psi(\vec{r}_{ik} = 0)|^2. \quad (2)$$

Here the nuclear magnetic moments are small, so that the orientation of nuclear spins due to the weak geomagnetic field can be neglected. The orbital angular momentum of the radical electrons is assumed to be fixed and to contribute no dynamics, while $\sum_i \vec{S}_i \cdot \vec{r}_k = 0$ in the $m_s = 0$ subspace. Eliminating these terms yields a Hamiltonian

of the form

$$H = \sum_i \mu_B \vec{B} \cdot \vec{S}_i + \vec{V}_{\text{SR}}^{(i)} \cdot \vec{S}_i + \sum_{i,k} \frac{\mu_0}{4\pi} (2\mu_B \frac{\mu_I}{I}) \vec{I}_k \cdot \vec{S}_i \frac{1}{|r_{ik}|^3} + \sum_{i,k_i} \frac{\mu_0}{4\pi} (2\mu_B \frac{\mu_I}{I}) \vec{I}_{k_i} \cdot [\frac{\vec{L}_i - \vec{S}_i}{|r_{ik_i}|^3} + \frac{8\pi}{3} |\psi(\vec{r}_{ik_i} = 0)|^2] \quad (3)$$

where the interaction of each electron with its nearest neighbor nuclei (indexed by k_i) has been separated from its interaction with the more distant nuclei of the surrounding bath.

An electron's interaction $\vec{V}_{\text{SR}}^{(i)} \cdot \vec{S}_i$ with its immediate surroundings may rival or exceed the strength of the Zeeman interaction $\vec{B} \cdot \vec{S}_i$. By lifting the degeneracy between $|\uparrow\downarrow\rangle$ and $|\downarrow\uparrow\rangle$, such interactions drive the coherent oscillation between singlet and triplet necessary for the radical pair model. As the precise receptor or receptors involved in the avian compass have not been identified (see [23–25] for candidates), the magnitude of this effect is unknown, although the narrow range of frequencies causing disorientation suggests that it is weak [24]. In the absence of a known receptor, this paper replaces the Zeeman and short range terms with $B_z \Delta\mu/2(|\uparrow\downarrow\rangle\langle\uparrow\downarrow| - |\downarrow\uparrow\rangle\langle\downarrow\uparrow|)$, where B_z is the magnetic field component in some direction preferred by the molecule and $\Delta\mu$ reflects the differences in the effective magnetic moment between the two electrons once this interaction is taken into account.

Decoherence between spin states of the radical pair occurs due to hyperfine interactions with the surrounding nuclei. Particularly important in this interaction is the form of the decoherence – the set of preferred states between which decoherence occurs. Both the form and the rate of decoherence are determined by the geometry of the excited state. Due to the r^{-3} dependence of the hyperfine interaction, distant electrons will interact with effectively distinct reservoirs, while electrons in close proximity will have an interaction which may be written as the sum of a symmetric term

$$\sum_k (\frac{2}{|R_k|^3}) A \vec{I}_k \cdot \vec{S} \quad (4)$$

and an antisymmetric term

$$\sum_k (\frac{3|r_{12}|\cos(\theta)}{|R_k|^4}) A \vec{I}_k \cdot \Delta\vec{S}, \quad (5)$$

where $|r_{12}|$ is the distance between the electrons, $A = \frac{\mu_0}{4\pi} (2\mu_B \frac{\mu_I}{I})$, $\vec{S} = \vec{S}_1 + \vec{S}_2$, $\Delta\vec{S} = \vec{S}_1 - \vec{S}_2$ and θ is the angle between \vec{r}_{12} and \vec{R}_k .

If the nucleus is assumed to be in thermal equilibrium with a local reservoir, a master equation for the decay of electronic coherence due to the hyperfine interaction may be found by tracing over the nuclear and environmental

degrees of freedom in the density matrix equations of motion for the full system. Working in the interaction picture,

$$\frac{\partial}{\partial t} \rho_{s+n+\epsilon}^I = - \int_0^\infty d\Delta t [V^I(t), [V^I(t-\Delta t), \rho_{s+n+\epsilon}^I(t-\Delta t)]], \quad (6)$$

where $H_0^{n+\epsilon}$ gives the interaction of the nucleus with the bath, H_0^s is the Zeeman Hamiltonian for the radical pair, $H_0 = H_0^s + H_0^{n+\epsilon}$, and $H = H_0 + V$. Here V can be either the symmetric or antisymmetric part of the hyperfine interaction. The short time evolution of the density matrix in Eq. 6 is given by

$$\rho^I(t + \Delta t) = e^{-iH_0\Delta t} e^{iH\Delta t} \rho^I(t) e^{-iH\Delta t} e^{iH_0\Delta t}. \quad (7)$$

Using the Born approximation, the effects of the radical pair interacting with the nucleus can be separated from the effects of the nucleus interacting with the bath. The form of the nucleus's interaction with the local bath is unknown, but assumed to drive the system toward a Markovian thermal equilibrium, with

$$\text{Tr}_\epsilon e^{-iH_0^{n+\epsilon}\Delta t} \rho_{n+\epsilon}(t) e^{iH_0^{n+\epsilon}\Delta t} = \sum_k |k\rangle \langle k| P_k \delta(\Delta t), \quad (8)$$

where $\{|k\rangle\}$ is some basis preferred by the interaction and P_k the probability of state $|k\rangle$ at thermal equilibrium. Meanwhile, the evolution of the density matrix due to H_0 and V can be found using the split operator method [26], so that $e^{iH\Delta t}$ can be approximated by $e^{iH_0\Delta t/2} e^{iV\Delta t} e^{iH_0\Delta t/2}$ and

$$\rho(t - \Delta t) = U(\Delta t) \rho(t) U(-\Delta t), \quad (9)$$

where $U(\Delta t) = e^{-iH_0\Delta t/2} e^{iV\Delta t} e^{iH_0\Delta t/2}$.

Substituting Eqs. 8 and 9 into Eq. 6 and tracing over environmental and nuclear degrees of freedom will now give a master equation for the decoherence due to V . For noncommuting H_0 and V , the oscillating exponential operators of Eq. 6 will result in a time integral containing many fourier components, while the rapid decay of nuclear spin coherence in Eq. 8 will contribute a delta function in time. The time integral can be evaluated by noting that

$$\int_0^\infty dt e^{i\omega t} \delta(t) = \frac{1}{|\omega|} \lim_{k \rightarrow \infty} \int_0^\infty d(\omega t) e^{i\omega t} k e^{-k|\omega t|} = \frac{1}{|\omega|}, \quad (10)$$

so that slowly oscillating terms give a larger contribution than rapidly oscillating terms. In the limit of a weak magnetic field, $e^{iH_0\Delta t} \approx 1$ over short times, and Eq. 6 becomes

$$\frac{\partial}{\partial t} \rho_{s+n+\epsilon} = - \int_0^\infty d\Delta t \delta(\Delta t) [V, [V, e^{iV\Delta t} \rho_{s+n+\epsilon} e^{-iV\Delta t}]]. \quad (11)$$

Eq. 11 can be evaluated by diagonalizing V . To this end, matrix elements of the form $\vec{I} \cdot \vec{S}$ can be evaluated using the Clebsch-Gordan expansion

$$|(j_1 j_2) JM\rangle = \sum_{m_1=-j_1}^{j_1} \sum_{m_2=-j_2}^{j_2} |j_1 m_1 j_2 m_2\rangle \langle j_1 m_1 j_2 m_2 | JM\rangle \quad (12)$$

and the identity

$$\vec{L}_1 \cdot \vec{L}_2 = \frac{1}{2} [\vec{J}^2 - \vec{L}_1^2 - \vec{L}_2^2], \quad (13)$$

where $\vec{J} = \vec{L}_1 + \vec{L}_2$ and J^2, J_z, \vec{L}_1^2 , and \vec{L}_2^2 are conserved by the interaction. Nonzero matrix elements of $\vec{I} \cdot \vec{S}$ are given in Table I.

$$\begin{aligned} \langle 1, 1; \uparrow | \vec{I} \cdot \vec{S} | 1, 1; \uparrow \rangle &= 1/2 \\ \langle 1, -1; \downarrow | \vec{I} \cdot \vec{S} | 1, -1; \downarrow \rangle &= 1/2 \\ \langle 1, 0; \uparrow | \vec{I} \cdot \vec{S} | 1, 1; \downarrow \rangle &= 1/\sqrt{2} \\ \langle 1, 1; \downarrow | \vec{I} \cdot \vec{S} | 1, 0; \uparrow \rangle &= 1/\sqrt{2} \\ \langle 1, 0; \downarrow | \vec{I} \cdot \vec{S} | 1, -1; \uparrow \rangle &= 1/\sqrt{2} \\ \langle 1, -1; \uparrow | \vec{I} \cdot \vec{S} | 1, 0; \downarrow \rangle &= 1/\sqrt{2} \\ \langle 1, 1; \downarrow | \vec{I} \cdot \vec{S} | 1, 1; \downarrow \rangle &= -1/2 \\ \langle 1, -1; \uparrow | \vec{I} \cdot \vec{S} | 1, -1; \uparrow \rangle &= -1/2 \end{aligned}$$

TABLE I. Nonzero matrix elements of $\vec{I} \cdot \vec{S}$ for states $|S, m_S; m_I\rangle$, from Equations 12 and 13.

It can now be seen that the symmetric- and anti-symmetric parts of the hyperfine interaction cause decoherence between different sets of preferred states. For the symmetric term, $\vec{S} = \vec{S}_1 + \vec{S}_2$, so that states $|s\rangle$ and $|t\rangle$ are eigenstates of the interaction with eigenvalues $|\bar{s}, \bar{m}\rangle = |0, 0\rangle$ and $|1, 0\rangle$. For the antisymmetric $\Delta\vec{S} = \vec{S}_1 - \vec{S}_2$, states $|\uparrow\downarrow\rangle$ and $|\downarrow\uparrow\rangle$ are eigenstates with eigenvalues $|\Delta s, \Delta m_s\rangle = |1, 1\rangle$ and $|1, -1\rangle$. Thus, the geometry of the excited state will determine the basis set in which off diagonal elements decay most rapidly. Substituting $V = \alpha \vec{I} \cdot \vec{S}$ into Eq. 11 yields an exponential rate of decay for the off diagonal elements in the preferred basis

$$\dot{\rho}_{1, m_i; 2, m_i}^I = -\frac{2}{3} \alpha \rho_{1, m_i; 2, m_i}^I \quad (14)$$

Although beyond the scope of the current paper, this analysis may be used to describe dynamics in the full spin space of the radical pair, as well as the case when $B \neq 0$. In the limit of strong magnetic fields, applicable to many laboratory experiments testing the radical pair model, the rate of decoherence goes as $\frac{V^2}{B}$ rather than V , while in the zero field limit the $m_s = 0$ subspace may lose population due to spin exchange with the surrounding nuclei. As $\mu_B \gg \mu_I$, the latter process is off resonant for even weak magnetic fields and has been neglected.

The loss of coherence due to the spin bath as a whole can be found via a spatial integral assuming a constant

density of nuclei per unit volume, so that

$$\bar{\Gamma} = 4\pi \int_{R_{\min}}^{R_{\max}} r^2 dr \bar{\lambda}(r) \quad (15)$$

and

$$\Delta\Gamma = 2\pi \int_0^\pi \sin(\theta) d\theta \int_{R_{\min}}^{R_{\max}} r^2 dr \Delta\lambda(r), \quad (16)$$

where $\bar{\lambda}(r) = \frac{4}{3}Ar^{-3}$, $\Delta\lambda(r, \theta) = 2A|r_{12}|\cos\theta r^{-4}$, and $A = \frac{\mu_0}{4\pi}(2\mu_B \frac{\mu_I}{T})$.

In Eqs. 15, the formal divergence of the $\bar{\Gamma}$ integral is cut off by assuming a slow gaussian decay term in addition to the exponential decay from Eq. 14. If the decoherence due to a particular nucleus is given by $f_r(t) = e^{-\lambda(r)|t| - \sigma t^2}$, with σ small, then the Fourier transform of $f_r(t)$ is given by $\mathbb{F}[f_r(t)] \approx \mathbb{F}[e^{-\lambda(r)|t|}]$ for $\lambda(r) \gg \sigma$ and $\mathbb{F}[f_r(t)] \approx \mathbb{F}[e^{-\sigma t^2}]$ for $\sigma \gg \lambda(r)$. Using the Fourier convolution theorem,

$$\mathbb{F}[e^{-\bar{\Gamma}|t| - \sigma t^2}] \approx [\tilde{\Pi}_{k|\lambda(r_k) > \sigma} \mathbb{F}[e^{-\lambda(r_k)|t|}]] * [\tilde{\Pi}_{k|\lambda(r_k) < \sigma} \mathbb{F}[e^{-\sigma t^2}]] \quad (17)$$

where $\tilde{\Pi}$ is the convolution rather than the multiplicative product. Noting that $\mathbb{F}^{-1}[\mathbb{F}[e^{-\lambda_1|t|}] * \mathbb{F}[e^{-\lambda_2|t|}]] = e^{-(\lambda_1 + \lambda_2)|t|}$, the effect of the slow gaussian decoherence is to introduce a cutoff radius R_{\max} such that $\lambda(R_{\max}) = \sigma$, beyond which nuclei do not contribute to the exponential part of the decoherence.

For the purpose of modeling the avian compass, it is sufficient to model the exponential part of the bath decoherence using the Lindblad equation

$$\frac{\partial}{\partial t} \rho = i[H, \rho] + \sum_{\kappa=|s\rangle, |t\rangle, |\uparrow\downarrow\rangle, |\downarrow\uparrow\rangle} \Gamma_\kappa \mathcal{L}_\kappa[\rho], \quad (18)$$

where $\mathcal{L}_\kappa[\rho] = -\rho L_\kappa^\dagger L_\kappa - L_\kappa^\dagger L_\kappa \rho + 2L_\kappa \rho L_\kappa^\dagger$ is the Lindblad superoperator corresponding to projection operator $L_\kappa = |\kappa\rangle\langle\kappa|$ and $\Gamma_\kappa = \bar{\Gamma}/2$ for $|\kappa\rangle = |s\rangle$ or $|t\rangle$, while $\Gamma_\kappa = \Delta\Gamma/2$ for $|\kappa\rangle = |\uparrow\downarrow\rangle$ or $|\downarrow\uparrow\rangle$.

The evolution of the density matrix components can be found analytically by calculating the evolution due to H and $\bar{\Gamma}$ in the singlet/triplet basis, then transforming to the $|\uparrow\downarrow\rangle, |\downarrow\uparrow\rangle$ basis to include the effects of $\Delta\Gamma$. As in [21], differential equations for the density matrix components due to H and $\bar{\Gamma}$ are given by

$$\begin{aligned} \frac{d^2}{dt^2}(\rho_{ss} - \rho_{tt}) + \bar{\Gamma} \frac{d}{dt}(\rho_{ss} - \rho_{tt}) + (B_z \Delta\mu)^2(\rho_{ss} - \rho_{tt}) &= 0 \\ \frac{d^2}{dt^2}(\rho_{ts} - \rho_{st}) + \bar{\Gamma} \frac{d}{dt}(\rho_{ts} - \rho_{st}) + (B_z \Delta\mu)^2(\rho_{ts} - \rho_{st}) &= 0 \\ \frac{d}{dt}(\rho_{ts} + \rho_{st}) &= -\bar{\Gamma}(\rho_{ts} + \rho_{st}) \\ \frac{d}{dt}(\rho_{ss} + \rho_{tt}) &= 0. \end{aligned}$$

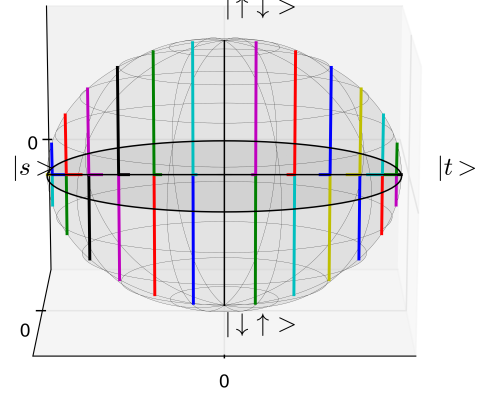


FIG. 1. (Color online) Decay of coherence in the Bloch sphere picture. For initially pure states, trajectories begin on the unit sphere before undergoing rapid decay of the z component and slow decay of the x and y components. Here, $\bar{\Gamma} = 10$ gauss $\cdot\mu_B$, $B = 50$ gauss, $\Delta\mu/\mu_B = 6 \times 10^{-4}$, $\Delta\Gamma = 0$ and $\Delta t = 0.1/\lambda_+$.

Here $(\rho_{ss} - \rho_{tt})$ and $(\rho_{ts} - \rho_{st})$ behave as damped harmonic oscillators, with time dependence

$$P(t) = Ae^{\lambda_+ t} + Be^{\lambda_- t}, \quad (19)$$

where

$$\lambda_{\pm} = \frac{-\bar{\Gamma} \pm \sqrt{\bar{\Gamma}^2 - 4(B_z \Delta\mu)^2}}{2}. \quad (20)$$

In the limit that $\bar{\Gamma} \gg |2B_z \Delta\mu|$, the system is strongly overdamped and the coherence terms will decay much more slowly than the base rate of dephasing, $\bar{\Gamma}$. It is this slow loss of coherence which allows for a biologically useful signal.

Transforming to a Bloch sphere representation gives a simple picture of the coherence dynamics in this system. If $|\uparrow\downarrow\rangle \rightarrow |0\rangle$ and $|\downarrow\uparrow\rangle \rightarrow 1$, then $(\rho_{ss} + \rho_{tt}) \rightarrow (\rho_{00} + \rho_{11}) = 1$, $(\rho_{ss} - \rho_{tt}) \rightarrow (\rho_{01} + \rho_{10}) = x\sigma_x$, $(\rho_{st} + \rho_{ts}) \rightarrow (\rho_{10} - \rho_{01}) = iy\sigma_y$, and $(\rho_{st} - \rho_{ts}) \rightarrow (\rho_{00} - \rho_{11}) = z\sigma_z$, where $\sigma_{x,y,z}$ are Pauli matrices. Decoherence due to the $\Delta\Gamma$ term is included by multiplying ρ_{10}, ρ_{01} by $e^{-\Delta\Gamma t}$. In the overdamped limit, $(\rho_{00} - \rho_{11})$ will decay rapidly as $e^{-\bar{\Gamma}t}$, so that the z coordinate of a point in the Bloch ball will rapidly decay to zero. However, both the x and y components are long lived, decaying as $e^{-\lambda_+ t}$. This decay is shown graphically in Figure 1. In spherical coordinates, the azimuthal angle θ is destabilized by interaction with the bath while the polar angle ϕ is stabilized, so that the symmetry group of the long-lived information is $U(1)$ rather than $SU(2)$.

In the radical pair model, creation of a purely singlet or purely triplet excited state places the Bloch vector

on the equator, where it has no rapidly decaying components. This gives a simple explanation for the long coherence times needed to be consistent with disorientation by a 15 nT oscillating field. However, in contrast to the original radical pair model, ϕ does not vary with time, so the system does not oscillate between singlet and triplet character. Rather, it is the decoherence between states $|\uparrow\downarrow\rangle$ and $|\downarrow\uparrow\rangle$ which generates an observable signal. For an initially pure singlet state in the $|\uparrow\downarrow\rangle$, $|\downarrow\uparrow\rangle$ basis, $\rho = \begin{pmatrix} 1/2 & 1/2 \\ 1/2 & 1/2 \end{pmatrix}$, and in the overdamped limit, $\dot{\rho} = -1/2 \begin{pmatrix} 0 & \lambda_+ + \Delta\Gamma \\ \lambda_+ + \Delta\Gamma & 0 \end{pmatrix}$, or $1/2 \begin{pmatrix} -\lambda_+ - \Delta\Gamma & 0 \\ 0 & \lambda_+ + \Delta\Gamma \end{pmatrix}$ in the singlet/triplet basis. Loss of coherence thus manifests itself as a transfer of population from the singlet to triplet state, at a rate which varies linearly with $\lambda_+ \approx (B_z \Delta\mu)^2 / \bar{\Gamma}$.

The dynamics derived above suggest a simple yet robust mechanism for a magnetic compass based upon an overdamped radical pair. Here the rate of decoherence, proportional to $|B_0 \cos(\theta)|^2$, provides the desired signal in the form of population transfer between the singlet and triplet states. If the triplet reaction rate is sufficient to prevent backwards transfer, the ratio of triplet to singlet byproducts is simply

$$R_{ts}(\theta) = \frac{\lambda_+ + \Delta\Gamma}{k_s} = \frac{|B_0 \Delta\mu \cos \theta|^2}{\bar{\Gamma} k_s} + \frac{\Delta\Gamma}{k_s}, \quad (21)$$

so that the ratio of triplet to singlet byproducts bears a simple relationship to the magnetic field orientation. Note that, as this signal is proportional to $\cos^2(\theta)$, this mechanism yields a compass which is sensitive to the orientation of magnetic field lines but not their polarity, consistent with behavioral experiments.

While the identity of the compass molecule remains unknown, some general design considerations may be inferred. Using Eq. 21, the sensitivity of the compass mechanism may be found by calculating the contrast between North/South and East/West alignment

$$\text{contrast} = \frac{R_{ts}(0) - R_{ts}(\pi/2)}{R_{ts}(0) + R_{ts}(\pi/2)} = \frac{(B_0 \Delta\mu)^2}{2\Delta\Gamma\bar{\Gamma} + (B_0 \Delta\mu)^2}. \quad (22)$$

Here the contrast depends upon the ratio of $\Delta\Gamma\bar{\Gamma}$ and $B_0 \Delta\mu$. Because the overdamped limit requires that $\bar{\Gamma}^2 \gg (B_0 \Delta\mu)^2$, a sensitive compass will require that $\Delta\Gamma$ be very small or even zero. Thus, the compass molecule may involve an excited state with a geometry which minimizes the antisymmetric part of the hyperfine interaction, or else a large region where water molecules are excluded, so that R_{min} in Eq. 16 is large.

A second design consideration relates to the singlet reaction rate, k_s . As seen in Eqs. 21 and 22, k_s is a free parameter which controls the visibility of the $R_{ts}(\theta)$ signal without affecting the sensitivity of the compass

mechanism as a whole. Because the rate of dephasing, and triplet formation goes as the square of the magnetic field strength, an ability to enhance or inhibit k_s would allow a migratory animal to use the same biochemical pathway for orientation regardless of the local magnetic field strength, while a static k_s would yield an optimal signal at some predetermined field strength.

The light-activated radical pair compass is a unique example of an intrinsically quantum mechanical process which survives and even depends upon a strong interaction between the system and the surrounding bath. Contrary to expectation, the interplay between coherent Hamiltonian evolution and bath-induced decoherence stabilizes part of the quantum information, allowing an organism to sense the orientation of the weak geomagnetic field. The avian compass, then, reflects a simple model system for the largely unexplored role of quantum mechanics in biology.

-
- [1] W. Wiltschko and R. Wiltschko, *Journal of Comparative Physiology A: Neuroethology, Sensory, Neural, and Behavioral Physiology*, **191**, 675 (2005).
 - [2] R. Muheim, *Photobiology*, 465 (2008).
 - [3] R. Wiltschko, I. Schiffner, P. Fuhrmann, and W. Wiltschko, *Current Biology*, **20**, 1534 (2010).
 - [4] L. Wu and J. Dickman, *Current Biology* (2011).
 - [5] L. Wu and J. Dickman, *Science* (2012).
 - [6] W. Wiltschko, R. Wiltschko, and T. Ritz, *Procedia Chemistry*, **3**, 276 (2011).
 - [7] T. Ritz, *Procedia Chemistry*, **3**, 262 (2011).
 - [8] S. Johnsen and K. Lohmann, *Nature Reviews Neuroscience*, **6**, 703 (2005).
 - [9] K. Able, *The condor*, **97**, 592 (1995).
 - [10] W. Wiltschko, K. Stapput, P. Thalau, and R. Wiltschko, *Naturwissenschaften*, **93**, 300 (2006).
 - [11] T. Ritz, P. Thalau, J. Phillips, R. Wiltschko, and W. Wiltschko, *Nature*, **429**, 177 (2004).
 - [12] K. Schulten, C. Swenberg, and A. Weller, *Zeitschrift für Physikalische Chemie*, **111**, 1 (1978).
 - [13] T. Ritz, S. Adem, and K. Schulten, *Biophysical journal*, **78**, 707 (2000).
 - [14] I. Kominis *et al.*, *Physical Review-Section E-Statistical Nonlinear and Soft Matter Physics*, **80**, 56115 (2009).
 - [15] W. Wiltschko and R. Wiltschko, *Journal of Experimental Biology*, **199**, 29 (1996).
 - [16] E. Gauger, E. Rieper, J. Morton, S. Benjamin, and V. Vedral, *Arxiv preprint arXiv:0906.3725* (2009).
 - [17] K. Kavokin, *Bioelectromagnetics*, **30**, 402 (2009).
 - [18] J. Cai, G. Guerreschi, and H. Briegel, *Physical review letters*, **104**, 220502 (2010).
 - [19] A. Johnson, J. Petta, J. Taylor, A. Yacoby, M. Lukin, C. Marcus, M. Hanson, and A. Gossard, *Nature*, **435**, 925 (2005).
 - [20] J. Petta, A. Johnson, J. Taylor, E. Laird, A. Yacoby, M. Lukin, C. Marcus, M. Hanson, and A. Gossard, *Science*, **309**, 2180 (2005).
 - [21] Z. Walters, *Quantum Physics Letters*, **1**, 21 (2012).
 - [22] G. Woodgate, *Elementary atomic structure* (Oxford Uni-

- versity Press, USA, 1983).
- [23] M. Liedvogel and H. Mouritsen, Journal of The Royal Society Interface, **7**, S147 (2010).
 - [24] H. Hogben, O. Efimova, N. Wagner-Rundell, C. Timmel, and P. Hore, Chemical Physics Letters, **480**, 118 (2009).
 - [25] C. Nießner, S. Denzau, J. Gross, L. Peichl, H. Bischof, G. Fleissner, W. Wiltchko, and R. Wiltchko, PloS one, **6**, e20091 (2011).
 - [26] A. Bandrauk and H. Shen, Chemical physics letters, **176**, 428 (1991).